

# QUANTUM ENTANGLEMENT TREES: OPTIMIZING QUANTIZED MATRIX QUANTIZATION VIA ELEMENT REPLACEMENT AND RESIDUAL CLUSTERING

**Yanshu Wang**

Peking University, Beijing, China  
yanshuwang@pku.edu.cn

**Wang Li**

Peking University, Beijing, China  
2401210642@stu.pku.edu.cn

**Tong Yang**

Peking University, Beijing, China  
yangtong@pku.edu.cn

## ABSTRACT

The matrix quantization entails representing matrix elements in a more space-efficient form to reduce storage usage, with dequantization restoring the original matrix for use. We formulate the Quantization Error Minimization (QEM) problem as minimizing the distance between a matrix before and after quantization, under the condition that the quantized matrix occupies the same memory space. Matrix quantization is crucial in various applications, including Large Language Models (LLMs) weight quantization, vector databases, KV cache quantization, graph compression, and image compression. Recent advancements in LLMs, such as GPT-4 and BERT, have highlighted the importance of matrix compression due to the large size of parameters and KV cache, which are stored as matrices.

We propose Quantum Entanglement Trees (QET) to address the QEM problem by leveraging the local orderliness of matrix elements, involving iterative element swapping to form a locally ordered matrix. This matrix is then grouped and quantized by columns. To enhance QET, we introduce two optimizations: further quantizing residuals to reduce MSE, and using masking and batch processing to accelerate the algorithm.

Experimental results demonstrate that QET can effectively reduce MSE to 12.3% of the original value at the same compression ratio, outperforming the best baseline algorithms. Our contributions include the abstraction of the QEM problem, the design of the QET algorithm, and the proposal of two optimizations to improve accuracy and speed.

## 1 INTRODUCTION

The matrix quantization entails representing the elements of a matrix in a more space-efficient form to reduce its storage usage. Dequantization, on the other hand, is the process during usage where the original matrix is restored from the quantized matrix using a restoration algorithm. We formulate the Quantization Error Minimization (QEM) problem as the task of minimizing the distance between a matrix before and after quantization in high-dimensional space, under the condition that the quantized matrix occupies the same space.

Matrix quantization is widely employed across diverse applications, including Large Language Models (LLMs) weight quantization (Dettmers et al. (2024); Lin et al. (2024); Shao et al. (2023); Xiao et al. (2023)), vector database (Xu et al. (2018); Jegou et al. (2010)), LLM k-v cache quantization (Liu et al. (2024); Zhang et al. (2024); Hooper et al. (2024); Kawakibi Zuhri et al. (2024); Duanmu et al. (2024); Yue et al. (2024); Lee et al. (2024); Adnan et al. (2024)), graph compression (Brisaboa et al. (2009); Claude & Ladra (2011)), and image compression (Yu et al. (2018); Ning et al. (2016)).

Specifically, the recent advancements in Large Language Models (LLMs) have made matrix compression even more critical. Large Language Models (LLMs) have revolutionized the field of natural language processing (NLP), enabling significant advancements in tasks such as machine translation, text generation, and sentiment analysis. These models, characterized by their large-scale neural network architectures and vast training datasets, have shown remarkable capabilities in understanding and generating human language. The advent of LLMs, such as OpenAI’s GPT-4 (Achiam et al. (2023)), and BERT (Devlin et al. (2018)) by Google, has pushed the boundaries of what machines can achieve in linguistic tasks, providing near-human performance in various applications. The parameters and KV cache in Large Language Models are very large in size. For instance, GPT-2 contains 1.5 billion parameters (Solaiman et al. (2019)), whereas GPT-3 has expanded to 175 billion parameters (Brown et al. (2020)). Additionally, the KV cache accounts for over 30% of GPU memory during deployment, compared to the 65% occupied by the parameters (Kwon et al. (2023)). Both the parameters and KV cache are stored in the form of matrices. GPTQ (Frantar et al. (2022)) and SqueezeLLM (Kim et al. (2023)) directly address the QEM problem by treating it as the optimization objective for quantizing parameters and the KV cache. Therefore, the abstracted scientific problem of QEM is highly significant.

There has been a growing literature on the matrix quantization. The first category of methods focuses on independently compressing the elements of a matrix for each specific scenario. Examples of such techniques include LLM.int8 (Ge et al. (2013)), Optimal Brain Damage (LeCun et al. (1989)), GPTQ (Frantar et al. (2022)), AWQ (Lin et al. (2023)), SmoothQuant (Xiao et al. (2023)), and OmniQuant (Shao et al. (2023)). The second category groups matrix elements by columns and then applies quantization to each group. Relevant works in this category include product quantization (PQ) (Jegou et al. (2010)), optimized product quantization (OPQ) (Ge et al. (2013)), locally optimized product quantization (LOPQ) (Kalantidis & Avrithis (2014)), and SqueezeLLM (Kim et al. (2023)). The first category of work can be summarized as utilizing outliers and the importance of elements in specific scenarios to improve the RTN (Round-To-Nearest)<sup>1</sup> (Gray & Neuhoff (1998)) algorithm. The second category focuses on enhancements to PQ algorithms. The primary drawback of the first category is that it does not consider the correlation between elements, instead independently quantizing and storing elements. Conversely, the second category fails to account for the relative order of elements.

In our research, we observed that the order of elements has a significant impact on the quantization outcome. Intuitively, consider a matrix  $\begin{bmatrix} 1 & 2 \\ 2 & 1 \end{bmatrix}$ . To losslessly quantize this matrix (with MSE=0), two vectors, [1, 2] and [2, 1], are required. However, if the matrix is reordered to  $\begin{bmatrix} 1 & 2 \\ 1 & 2 \end{bmatrix}$ , it can be losslessly quantized using just a single vector, [1, 2].

Using these ideas, we propose Quantum Entanglement Trees (QET) to address the QEM problem in matrix quantization. The core idea of QET is to leverage the local orderliness of matrix elements to optimize the QEM problem. The design involves swapping adjacent elements of the matrix to form a new, locally ordered matrix. To cover a broader range, we can perform further element swapping on the initially locally ordered matrix, similar to the approach of receptive field used in convolutional neural networks (LeCun et al. (1998)). This step can be repeated for multiple iterations. The newly ordered matrix is then grouped by columns, with each group being quantized.

Additionally, we propose two optimization algorithms based on the basic QET. First, the residuals between the original and quantized matrices can be further quantized to enhance the accuracy of the results. Second, since the iterative swapping operations can slow down the algorithm, we introduce optimization techniques based on masking and batch processing to accelerate the QET.

We evaluate QET on multiple datasets. Experimental results demonstrate that our method can effectively reduce the MSE to 12.3% of the original value at the same compression ratio, compared to the best baseline algorithm, which achieves an MSE of XXXX%.

We summarize our contributions below.

<sup>1</sup>RTN (Round-To-Nearest) is an algorithm that quantizes elements by rounding each value to its nearest representable level.

- Abstracted a problem: We abstracted the Quantization Error Minimization (QEM) problems from various application scenarios.
- Designed an algorithm: We developed the Quantum Entanglement Trees (QET) algorithm, leveraging the concept of local orderliness to optimize the QEM problem.
- Proposed two optimizations: We introduced the use of residuals to reduce MSE and employed batch processing techniques to accelerate QET algorithm.

## 2 PROBLEM SETTING

In this section, we formally define the Quantization Error Minimization (QEM) problem and analyze the impact and feasibility of rearranging matrix elements prior to quantization.

**QEM Problem:** we denote the matrix to be quantized as  $X$ , the quantized matrix as  $X^q$ , and the matrix obtained by dequantizing  $X^q$  as  $X'$ . Both  $X$  and  $X'$  are  $n \times d$  dimensional, but the dimensions of  $X^q$  depend on the quantization algorithm. The elements of these matrices are denoted as  $x_{(i,j)}$ ,  $x_{(i,j)}^q$ , and  $x'_{(i,j)}$ , respectively. The memory occupied by a matrix is denoted as `memory()`, and the memory constraint as `mem_constrain`.

**Definition 1** (Quantization Error Minimization (QEM) Problem). The Quantization Error Minimization (QEM) problem is defined as the task of minimizing the combined objective of the Mean Squared Error (MSE) and the memory size of the quantized matrix:

$$\text{minimize } \text{MSE}(X, X') + \lambda \cdot \text{memory}(X^q),$$

where

$$\text{MSE}(X, X') = \frac{1}{n \cdot d} \sum_{i,j} \left( x_{(i,j)} - x'_{(i,j)} \right)^2,$$

$\lambda$  is a regularization parameter that balances the trade-off between minimizing the MSE and the memory usage of the quantized matrix.

Subject to the condition that the quantized matrix occupies the same space:

$$\text{memory}(X^q) \leq \text{mem\_constrain},$$

**Rearranging matrix elements:** Our idea is to rearrange the matrix elements before quantization. Let the quantization algorithm be denoted as `quant()` and the rearrangement algorithm as `rearrange()`. Previously, the quantized matrix was obtained as  $X^q = \text{quant}(X)$ , whereas in our rearrangement approach, it is obtained as  $X^q = \text{quant}(\text{rearrange}(X))$ . Therefore, the rearrangement algorithm only affects the quantization if the quantization method is order-sensitive. For instance, order-insensitive algorithms like RTN do not benefit from rearrangement because RTN processes each element independently, while order-sensitive algorithms like PQ can be optimized through rearrangement.

However, finding the optimal arrangement requires exploring a large search space. Specifically, for an  $n \times d$  matrix, there are  $(n!)^d$  possible rearrangements. Therefore, searching the entire space is impractical, and we need heuristic algorithms to prioritize exploring more promising regions of the search space.

## 3 METHODS

The core idea of Quantum Entanglement Trees (QET) is to leverage the local orderliness of matrix elements by rearranging adjacent elements to optimize the matrix quantization algorithm. Additionally, multiple iterations are used to expand the algorithm's swapping field. We begin by describing the basic version of this idea and then propose two optimizations for the basic algorithm.

### 3.1 BASIC ALGORITHM

The steps and design of the QET algorithm are illustrated in Figure 2. The figure provides a conceptual overview of the Quantum Entanglement Trees (QET) algorithm.

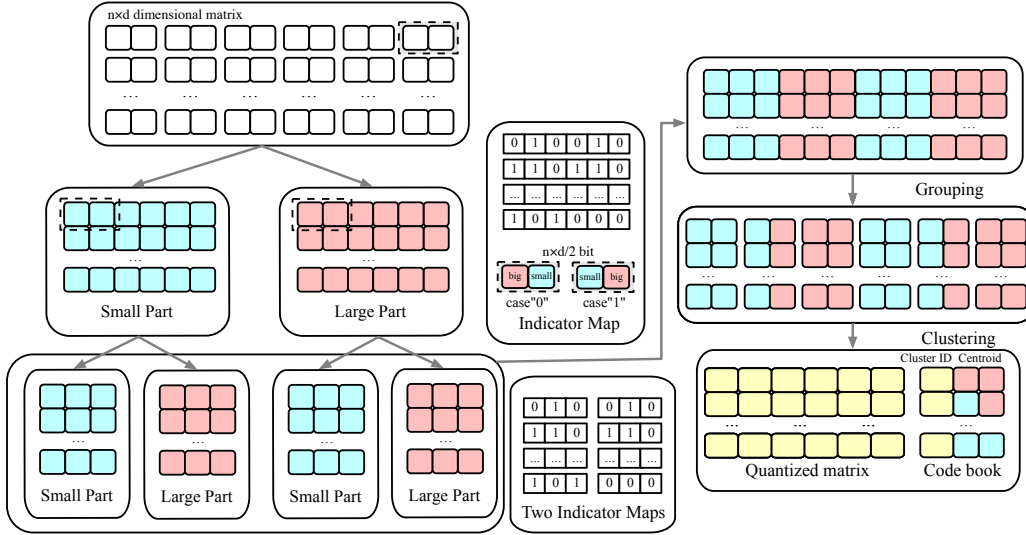


Figure 1: QET algorithm.

On the left side of the figure, the process of rearranging matrix elements through multiple iterations in the QET is depicted. This iterative procedure involves comparing adjacent elements and ensuring that adjacent elements are not placed in the same matrix. This separation of adjacent elements into different matrices is conceptually similar to quantum entanglement, hence the name "Quantum Entanglement Trees." The QET algorithm performs multiple iterations, with each iteration comparing adjacent elements and splitting them based on their values. This approach is based on two observations. First, the local orderliness of the matrix can enhance the regularity of matrix elements, thereby improving compression efficiency. Second, multiple iterations allow the orderliness to cover a larger number of elements. For instance, adjacent elements after the first iteration might be non-adjacent in the original matrix. This iterative process, similar to that of convolutional neural networks, extends the "receptive field" to cover more elements.

On the right side of the figure, the QET compression process is shown. After the elements have been rearranged, the algorithm groups the sub-matrices, followed by clustering to determine the centroids. These centroids are used to quantize the matrix. The final quantized matrix, codebook, and indicator maps are the outputs of the QET algorithm. This divide-and-conquer compression method is based on an observation: by splitting the matrix, the expressive power can be increased under a fixed storage constraint. For example, if the matrix is divided into  $m$  blocks, each with  $c$  centroids, the entire matrix can express  $c^m$  centroids while only storing  $c \times m$  centroids. Without splitting, storing  $c^m$  centroids would be required.

### 3.2 QET QUANTIZATION

The proposed QET Algorithm is designed to optimize the quantization of a matrix  $X \in \mathbb{R}^{n \times d}$  by leveraging local orderliness. The algorithm proceeds in four key steps, as shown in Algorithm 3.2.1:

**Step 1: Initial Partitioning.** The algorithm starts by comparing each adjacent pair of elements  $(x_{i,j}, x_{i,j+1})$  in the input matrix  $X$ . Based on the comparison of these elements, the smaller value is placed into matrix  $S$  and the larger into matrix  $L$ . Concurrently, an Indicator Map  $I$  is generated, where a 0 denotes that the smaller element is on the left and a 1 denotes it is on the right. This process results in the creation of two matrices,  $S$  and  $L$ , which collectively represent the initial partitioning of the original matrix  $X$ .

**Step 2: Recursive Partitioning.** Following the initial partitioning, the algorithm undertakes a recursive partitioning process. Starting from  $k = 1$ , the matrices  $S_k^i$  and  $L_k^{i,2}$  derived from the previous iteration (for  $i = 1, 2, \dots, 2^{k-1}$ ) are further partitioned based on their sizes. In each iteration, a new Indicator Map  $I_{k+1}$  is generated and then merged with the existing Indicator Maps. This recursive process continues until the predefined number of iterations  $l$  is reached. The resulting Indicator Maps  $I_1, I_2, \dots, I_l$  are stored in the set  $IM$ . The final matrices  $S_l$  and  $L_l$  are combined to form a new matrix  $X^*$ , which represents a locally ordered version of the original matrix.

**Step 3: Subspace Grouping.** After constructing the matrix  $X^*$ , it is divided into subspaces  $\{G_i\}$ , where  $i = 1, 2, \dots, m$ . This division is based on the local ordering of elements, which facilitates more effective clustering and quantization in the subsequent steps.

**Step 4: Clustering and Quantization.** In the final step, each subspace  $G_k$  (for  $k = 1, 2, \dots, m$ ) is clustered to determine a set of centroids  $C_k = \{\mathbf{c}_j\}$ . Each vector  $\mathbf{g}_i$  within the subspace is then quantized by assigning it to the nearest centroid. This process results in the quantized matrix  $X^q$ . The output of the algorithm includes the quantized matrix  $X^q$ , the codebook  $\mathbf{C}$  containing the centroids, and the Indicator Maps  $IM$ .

---

#### Algorithm 1 QET Quantization Algorithm

---

- 1: **Input:** Matrix  $X \in \mathbb{R}^{n \times d}$ ,  $m$  is the number of subspaces for quantization,  $l$  is the number of QET iterations.
- 2: **Output:** Quantized matrix  $X^q = \{X_{i,k}^q\}$  where  $i = 1, \dots, d$  and  $k = 1, \dots, m$ , Codebook  $\mathbf{C} = \{C_i\}$  where  $i = 1, \dots, m$ , and Indicator Maps  $IM = \{I_i\}$  where  $i = 1, \dots, l$
- 3: Initialize  $IM$  and  $X^q$  as empty
- 4: **Step 1: Initial Partitioning**
- 5: **for** each adjacent pair  $(x_{i,j}, x_{i,j+1})$  in  $X$  **do**
- 6:     **if**  $x_{i,j} > x_{i,j+1}$  **then**
- 7:          $S_{i,j} \leftarrow x_{i,j+1}, L_{i,j} \leftarrow x_{i,j}$
- 8:          $I(\frac{i}{2}, j) \leftarrow 0$
- 9:     **else**
- 10:          $S_{i,j} \leftarrow x_{i,j}, L_{i,j} \leftarrow x_{i,j+1}$
- 11:          $I(\frac{i}{2}, j) \leftarrow 1$
- 12:     **end if**
- 13: **end for**
- 14: **Step 2: Recursive Partitioning**
- 15:  $k \leftarrow 1$
- 16: **while**  $k \neq l$  **do**
- 17:     **for**  $i = 1$  to  $2^{k-1}$  **do**
- 18:         Apply size-based partitioning to  $S_k^i$  and  $L_k^i$
- 19:         Generate and merge new Indicator Maps into  $I_{k+1}$  for each partition
- 20:     **end for**
- 21:      $k \leftarrow k + 1$
- 22: **end while**
- 23: Store  $I_1, I_2, \dots, I_l$  into  $IM$
- 24:  $X^* \leftarrow S_l^1 \cup L_l^1 \cup S_l^2 \cup L_l^2 \cup \dots \cup S_l^{2^{l-1}} \cup L_l^{2^{l-1}}$   $\triangleright$  Combine the locally ordered parts from the final layer  $l$
- 25: **Step 3: Subspace Grouping**
- 26: Group the matrix  $X^*$  into subspaces  $\{G_i\}$  where  $i = 1, 2, \dots, m$
- 27: **Step 4: Clustering and Quantization**
- 28: **for** each vector  $\mathbf{g}_i$  in  $G_k$  (for  $k = 1, 2, \dots, m$ ) **do**
- 29:     Apply clustering to find centroids  $C_k = \{\mathbf{c}_j\}$
- 30:      $X_{i,k}^q \leftarrow \arg \min_{\mathbf{c}_j} \|\mathbf{g}_i - \mathbf{c}_j\|$   $\triangleright$  Quantize to nearest centroid within group
- 31: **end for**
- 32: **Return** Quantized matrix  $X^q$ , Codebook  $\mathbf{C}$ , and Indicator Maps  $IM$

---

<sup>2</sup>Since each level has multiple  $S$  and  $L$  matrices, we use the subscript to denote the iteration number and the superscript to denote the sequence within each iteration.

### 3.2.1 QET DEQUANTIZATION

The dequantization process, as described by the QET Dequantization Algorithm, aims to reconstruct the original matrix  $X'$  from its quantized version  $X^q$ . This process involves several key steps, as shown in Algorithm 3.2.1:

**Step 1: Dequantization Using Codebook.** The first step involves using the codebook  $\mathbf{C}$  to directly retrieve the original vectors corresponding to each quantized vector  $\mathbf{g}_i^q$  in the matrix  $X^q$ . For each vector  $\mathbf{g}_i^q$  in  $X_{i,k}^q$ , the algorithm assigns  $\mathbf{g}_i^q$  to the centroid  $\mathbf{c}_j$  from the codebook, where  $j$  is the index corresponding to the quantized vector. This step effectively reverses the quantization by mapping the quantized vectors back to their original forms using the codebook entries.

**Step 2: Reverse Subspace Grouping.** After mapping, the algorithm combines the dequantized subspaces  $\{G'_i\}$ , where  $i = 1, 2, \dots, m$ , into a single matrix  $X'^*$ . Each subspace  $G'_i$  contains the vectors  $\mathbf{g}_i^q$  corresponding to the original matrix entries. This step reconstructs the subspaces into a uniform matrix that is a preliminary version of the original matrix  $X'$ .

**Step 3: Reverse Recursive Partitioning and Final Reconstruction.** The final step involves reversing the recursive partitioning process that was applied during quantization. Starting from the last iteration  $k = l$ , the algorithm merges the matrices  $S_k$  and  $L_k$  based on the Indicator Maps  $I_k$  and the matrix  $X'^*$ . This merging process is iteratively applied from  $k = l$  down to  $k = 1$ , updating  $X'^*$  at each step to gradually reconstruct the original matrix structure. The final output of the algorithm is the reconstructed matrix  $X' \in \mathbb{R}^{n \times d}$ , which approximates the original matrix before quantization.

---

#### Algorithm 2 QET Dequantization Algorithm

---

- 1: **Input:** Quantized matrix  $X^q = \{X_{i,k}^q\}$ , where  $i = 1, \dots, d$  and  $k = 1, \dots, m$ ; Codebook  $\mathbf{C} = \{C_i\}$ , where  $i = 1, \dots, m$ ; and Indicator Maps  $IM = \{I_i\}$ , where  $i = 1, \dots, l$
  - 2: **Output:** Reconstructed matrix  $X' \in \mathbb{R}^{n \times d}$
  - 3: Initialize  $X'$  as empty
  - 4: **Step 1: Dequantization Using Codebook**
  - 5: **for** each vector  $\mathbf{g}_i^q$  in  $X_{i,k}^q$  **do**
  - 6:      $\mathbf{g}_i^q \leftarrow \mathbf{c}_j$ , where  $j$  corresponds to the codebook entry for  $\mathbf{g}_i^q$  ▷ Direct lookup from codebook
  - 7: **end for**
  - 8: **Step 2: Reverse Subspace Grouping**
  - 9: Combine subspaces  $\{G'_i\}$ , where  $i = 1, 2, \dots, m$ ,  $G'_i = \{\mathbf{g}_i^q\}$  for  $i = 1$  to  $n$ , to form  $X'^*$
  - 10: **Step 3: Reverse Recursive Partitioning**
  - 11:  $k \leftarrow l$
  - 12: **while**  $k \neq 0$  **do**
  - 13:     **for**  $i = 1$  to  $2^{k-1}$  **do**
  - 14:         Merge  $S_k^i$  and  $L_k^i$  based on  $I_k$  and  $X'^*$ , then update the results into  $X'^*$
  - 15:     **end for**
  - 16:      $k \leftarrow k - 1$
  - 17: **end while**
  - 18: **Return** Reconstructed matrix  $X'$
- 

### 3.3 OPTIMIZATIONS

In this section, we propose three optimizations: Residual Optimization (RO), Batch Processing Optimization (BPO), and Codebook Quantization Optimization (CQO). RO takes advantage of the fact that, after applying QET, the range of the data is relatively small, allowing for further optimization of the residual matrix and improvement of the MSE. On the other hand, BPO utilizes batch processing techniques to enhance processing speed. Since the codebook used in the QET algorithm occupies significant space, CQO further quantizes the codebook to improve space efficiency.

#### 3.3.1 RESIDUAL OPTIMIZATION

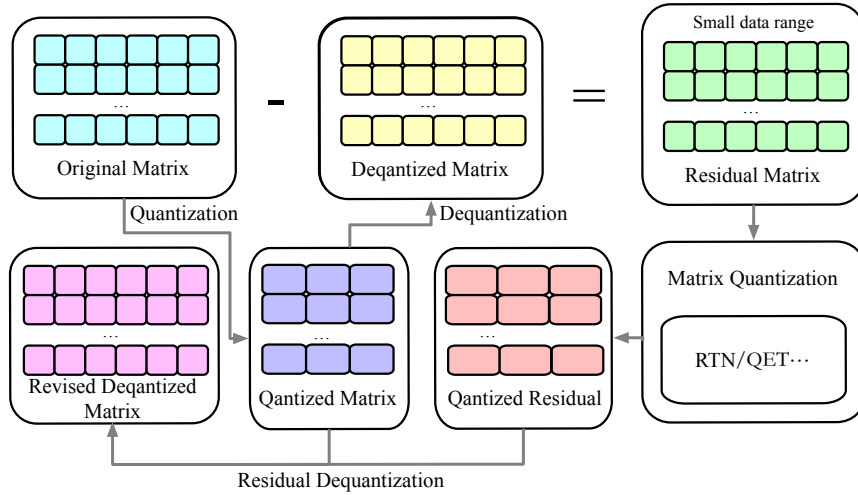


Figure 2: Residual Optimization Algorithm.

Residual Optimization (RO) is grounded in our observation that the data range of the quantized matrix is significantly reduced after applying the QET algorithm. As shown in Table 3.3, our experiments indicate that at a compression ratio of 16, the data range of the quantized matrix is reduced to 29.7% of the original matrix’s range. Moreover, with a compression ratio of 4, the data range of the quantized matrix is reduced to approximately 1.6% of the original matrix’s range.

Matrix quantization algorithms are more efficient at compressing matrix with a smaller data range; therefore, we propose Residual Optimization (RO). The RO algorithm, as depicted in Figure 3.3.1, begins with the quantization of the original matrix to produce a quantized matrix. This matrix is then dequantized to yield a dequantized matrix, which is subtracted from the original matrix to form a residual matrix. The residual matrix typically exhibits a significantly reduced data range, making it easier to compress. This residual matrix is then quantized using a chosen matrix quantization algorithm, such as RTN or QET.

During the dequantization process, the quantized residual is dequantized, and this dequantized residual is added back to the initially dequantized matrix to produce a revised dequantized matrix.

Table 1: Range Ratios, and Codebook(CB) Proportions in different compression ratios.

Compression Ratio	4.0	8.0	12.0	16.0
Range Ratio (%)	1.6	4.0	9.2	29.7
CB Proportion (%)	87.5	78.1	71.8	62.5

### 3.3.2 BATCH PROCESSING OPTIMIZATION

The key insight behind (Batch Processing Optimization) BPO is that by organizing and processing data in larger chunks or batches and enhancing the efficiency of the QET algorithm through batch processing and vectorization operations, the algorithm can more efficiently determine the relationships between elements, such as identifying smaller and larger parts or setting indicator maps.

In the original process, elements of the matrix are compared and sorted individually, leading to a sequential, element-by-element approach that can become computationally intensive as the matrix size increases. This method is not optimal for large-scale matrices.

BPO introduces a more advanced technique by processing matrix elements in parallel batches rather than sequentially. This parallelization allows the algorithm to handle multiple comparisons and sorting operations simultaneously, rather than one at a time. By doing so, it reduces the overall computational complexity and accelerates the entire quantization process.

### 3.3.3 CODEBOOK QUANTIZATION OPTIMIZATION (CQO)

The codebook occupies a significant portion of the space in the QET algorithm. As shown in Table 3.3, our experiments indicate that when the compression ratio is 16, the codebook occupies 62.5% of the total space, and when the compression ratio is 4, the codebook occupies 87.5% of the total space. Therefore, compressing the codebook can significantly reduce the space used by the algorithm. Our optimization mainly employs the RTN method to compress the codebook.

## 4 THEORETICAL GUARANTEES OF QET

In this section, we will first derive the MSE of the PQ and QET algorithms, then theoretically prove that the MSE of our QET algorithm is lower than that of the PQ algorithm.

**Theorem 1.** Suppose each element in the matrix is independently sampled from a normal distribution  $x_{(i,j)} \sim \mathcal{N}(\mu, \sigma)$ . After Quantized by the PQ algorithm, the MSE is as follows:

$$\text{MSE} = \sigma^2 - \frac{\sigma^2}{n_k}$$

$A_{ij} \sim \mathcal{N}(\mu, \sigma^2)$  independently and identically distributed

$B_{ij}$  cluster centroid matrix,  $n_k$  is the number of samples in the cluster

$C_{ij}$  residual matrix

$$E[C_{ij}] = E[A_{ij} - B_{ij}] = \mu - \mu = 0$$

$$\text{MSE} = \text{Var}[C_{ij}] = \text{Var}[A_{ij}] + \text{Var}[B_{ij}] - 2 \cdot \text{Cov}(A_{ij}, B_{ij})$$

$$= \sigma^2 + \frac{\sigma^2}{n_k} - 2 \cdot \text{Cov}(A_{ij}, B_{ij})$$

$$= \sigma^2 + \frac{\sigma^2}{n_k} - 2E \left[ (A_{ij} - \mu) \left( \frac{1}{n_k} \sum_{i=1}^{n_k} A_{ij} - \mu \right) \right]$$

$$= \sigma^2 + \frac{\sigma^2}{n_k} - 2 \left[ \frac{1}{n_k} E [(A_{ij} - \mu)^2] + \frac{1}{n_k} \sum_{i \neq i'} E [(A_{ij} - \mu)(A_{i'j} - \mu)] \right]$$

Since  $A_{ij}$  and  $A_{i'j}$  ( $i \neq i'$ ) are independent

$$= \sigma^2 + \frac{\sigma^2}{n_k} - 2 \cdot \frac{\sigma^2}{n_k}$$

$$\text{MSE} = \sigma^2 - \frac{\sigma^2}{n_k} \tag{1}$$

In this section, this paper will theoretically prove that the MSE of our HERA algorithm is lower than that of the PQ algorithm.

Suppose each element in the matrix is independently sampled from a normal distribution  $\mathcal{N}(\mu, \sigma)$ . After compression by the PQ algorithm, the process for calculating MSE is as follows:

$A_{ij} \sim \mathcal{N}(\mu, \sigma^2)$  independently and identically distributed

$B_{ij}$  cluster centroid matrix,  $n_k$  is the number of samples in the cluster

$C_{ij}$  residual matrix

$$E[C_{ij}] = E[A_{ij} - B_{ij}] = \mu - \mu = 0$$

$$MSE = \text{Var}[C_{ij}] = \text{Var}[A_{ij}] + \text{Var}[B_{ij}] - 2 \cdot \text{Cov}(A_{ij}, B_{ij})$$

$$= \sigma^2 + \frac{\sigma^2}{n_k} - 2 \cdot \text{Cov}(A_{ij}, B_{ij})$$

$$= \sigma^2 + \frac{\sigma^2}{n_k} - 2E \left[ (A_{ij} - \mu) \left( \frac{1}{n_k} \sum_{i=1}^{n_k} A_{ij} - \mu \right) \right]$$

$$= \sigma^2 + \frac{\sigma^2}{n_k} - 2 \left[ \frac{1}{n_k} E[(A_{ij} - \mu)^2] + \frac{1}{n_k} \sum_{i \neq i'} E[(A_{ij} - \mu)(A_{i'j} - \mu)] \right]$$

Since  $A_{ij}$  and  $A_{i'j}$  ( $i \neq i'$ ) are independent

$$= \sigma^2 + \frac{\sigma^2}{n_k} - 2 \cdot \frac{\sigma^2}{n_k}$$

$$= \sigma^2 - \frac{\sigma^2}{n_k} \quad (2)$$

For the HERA algorithm proposed in this paper, the MSE obtained using the HERA algorithm on a matrix with elements following a  $\mathcal{N}(\mu, \sigma^2)$  distribution is equivalent to the MSE obtained using the PQ algorithm on a matrix with elements following a distribution with variance  $0.682\sigma^2$ . According to formula equation 2 equation 3, the MSE of HERA is smaller than that of the PQ. The following discussion in this paper will explain why this equivalence holds.

For a Gaussian distribution, after applying element pairing in the HERA algorithm, the cumulative distribution function  $F_Y(y)$  of the elements on the right side of the matrix (the side storing the larger elements) satisfies:

$$F_Y(y) = P(Y \leq y) = P(\max(X_1, X_2) \leq y) = P(X_1 \leq y) \cdot P(X_2 \leq y)$$

Each  $X_i$  follows a normal distribution  $N(\mu, \sigma^2)$

$$F_Y(y) = \Phi\left(\frac{y-\mu}{\sigma}\right) \cdot \Phi\left(\frac{y-\mu}{\sigma}\right) = \left[\Phi\left(\frac{y-\mu}{\sigma}\right)\right]^2 = \frac{1}{4} \left[1 + \text{erf}\left(\frac{y-\mu}{\sigma\sqrt{2}}\right)\right]^2$$

Take the derivative of  $F_Y(y)$  :

$$f_Y(y) = \left[1 + \text{erf}\left(\frac{y-\mu}{\sigma\sqrt{2}}\right)\right] \cdot \frac{1}{\sqrt{2\pi}\sigma^2} \exp\left(-\frac{(y-\mu)^2}{2\sigma^2}\right)$$

The mean and variance of  $Y$  are given by:

$$E(Y) = \int_{-\infty}^{\infty} y \left[ 1 + \operatorname{erf} \left( \frac{y - \mu}{\sigma\sqrt{2}} \right) \right] \cdot \frac{1}{\sqrt{2\pi\sigma^2}} \exp \left( -\frac{(y - \mu)^2}{2\sigma^2} \right) dy$$

$$\operatorname{Var}(Y) = \int_{-\infty}^{\infty} (y - E(Y))^2 \left[ 1 + \operatorname{erf} \left( \frac{y - \mu}{\sigma\sqrt{2}} \right) \right] \cdot \frac{1}{\sqrt{2\pi\sigma^2}} \exp \left( -\frac{(y - \mu)^2}{2\sigma^2} \right) dy$$

Use numerical integration methods:

$$E(Y) = \mu + 0.564\sigma$$

$$\operatorname{Var}(Y) = 0.682\sigma^2 \tag{3}$$

Taking symmetry into account, the left side of the matrix also adheres to equation equation 3.

## 5 EXPERIMENTS

### 5.1 EXPERIMENT SETUP

**Dataset:** To evaluate the effectiveness of our proposed algorithm, we conducted experiments using one synthetic dataset and four real-world datasets: a synthetic normal distribution dataset, LLM weight dataset, KV cache dataset, Gist dataset, and Wiki dataset. Due to space constraints, we present the results for the synthetic normal distribution dataset and the LLM weight dataset in the main text. The results for the other datasets are provided in the appendix (Section ??). Below, we provide a detailed description of each dataset.

(1) Synthetic normal distribution dataset: This dataset was generated by drawing each element of the matrix from a truncated normal distribution with a mean of 0.5 and a standard deviation of 0.16. Additionally, one out of every ten thousand elements was replaced with an outlier value, randomly chosen between -100 and 100.

(2) LLM weight dataset: This dataset comprises weight matrices extracted from the large language model (LLM) LLaMA2 (Touvron et al. (2023)).

(3) KV cache dataset: The KV cache dataset is derived from the key-value pairs stored in the cache during inference in KV Quant (Hooper et al. (2024)). The key and value are stored in matrices, respectively.

(4) Gist dataset: The Gist dataset consists of feature vectors used for image recognition and retrieval tasks. GIST consists of the first 100k features extracted from the tiny image set (Torralba et al. (2008)). The dataset is also used in Jegou et al. (2010) and Oliva & Torralba (2001).

(5) Wiki dataset: The Wiki dataset (wik (2023)) contains document embeddings derived from Wikipedia articles. This dataset includes 256-dimensional vectors for a sample of 1 million Wikipedia entries.

**Platform and implementation:** We conducted our algorithm evaluations on a high-performance server equipped with an Intel Core i9-10980XE processor, featuring 18 cores and 36 threads, operating at a base frequency of 3.00 GHz. The server also includes 128GB of 3200MHz DDR4 memory and a 24.8MB L3 cache, providing robust computational capabilities. All algorithms were implemented in Python, using version 3.8.10. For each case, the experiment was repeated 100 times. In each repetition, matrices of the same size and from the same distribution were generated using different seeds.

**Metrics:** We primarily measure the accuracy and time consumption of the algorithm. We use MAE (Mean Absolute Error), MRE (Mean Relative Error), and MSE (Mean Squared Error) as accuracy

metrics. QTR (Quantization Time Ratio) and DTR (Dequantization Time Ratio) are used as time consumption metrics. Below, we introduce these metrics in detail.

Let  $x_{(i,j)}$  denote the elements of the original matrix to be quantized, and  $x'_{(i,j)}$  denote the elements of the dequantized matrix.

$$\text{MAE} = \frac{1}{n \cdot d} \sum_{i,j} |x_{(i,j)} - x'_{(i,j)}|, \quad \text{MSE} = \frac{1}{n \cdot d} \sum_{i,j} (x_{(i,j)} - x'_{(i,j)})^2$$

For time efficiency, we define the following metrics:

$$\text{QTR} = \frac{T_{\text{quant}}}{T_{\text{quant, baseline}}}, \quad \text{DTR} = \frac{T_{\text{dequant}}}{T_{\text{dequant, baseline}}}$$

In these equations,  $T_{\text{quant}}$  and  $T_{\text{dequant}}$  represent the time taken by the proposed algorithm to quantize and dequantize the data, respectively.  $T_{\text{quant, baseline}}$  and  $T_{\text{dequant, baseline}}$  refer to the corresponding times taken by the baseline algorithm.

**Comparative Algorithms:** For the abstract Quantization Error Minimization (QEM) problem, our comparative algorithms fall into two main categories. The first category involves independently compressing the elements of a matrix for each specific scenario, which can be abstracted as the RTN (Round-To-Nearest) algorithm. The second category groups matrix elements by columns and then applies quantization to each group. Related algorithms in this category include PQ, OPQ, and LOPQ. Therefore, our comparative algorithms are as follows: RTN (Round-To-Nearest) (Gray & Neuhoff (1998)), PQ (Product Quantization) (Jegou et al. (2010)), OPQ (Optimized Product Quantization) (Ge et al. (2013)), and LOPQ (Locally Optimized Product Quantization) (Kalantidis & Avrithis (2014)).

### Parameter Selection

In this section, we describe the parameter selection process for our HERA algorithm and compare its performance with the Optimized Product Quantization (OPQ) algorithm.

For Residual Optimization (RO), the large space required by RTN makes it infeasible for the algorithm to achieve high compression ratios. Therefore, in our experiments, we primarily use QET as the residual algorithm for RO.

Our QET algorithm involves a critical parameter, the number of centroids  $k_s$ . The selection of  $k_s$  is governed by the following memory constraint:

where:

- $k_s$  is the number of centroids,
- $d$  is the dimensionality of each sample,
- $n$  is the number of samples,
- $m$  is the number of subspaces,
- bitlength is the bit length used for encoding.

This constraint ensures that the total memory usage remains within the available memory limits. By carefully selecting  $k_s$ , we aim to optimize the performance of the HERA algorithm while adhering to memory constraints.

The Optimized Product Quantization (OPQ) algorithm was used as a benchmark for comparison. The OPQ algorithm was implemented with default parameters, providing a consistent basis for performance evaluation. The OPQ algorithm optimizes product quantization by adjusting the space partitioning and centroid assignments to minimize quantization error.

### Accuracy Measurement

We measure MAE, MRE and MSE on different numbers of subspaces to show the accuracy of HERA. The results for MAE, MRE and MSE for different number of subspaces are shown in Figures

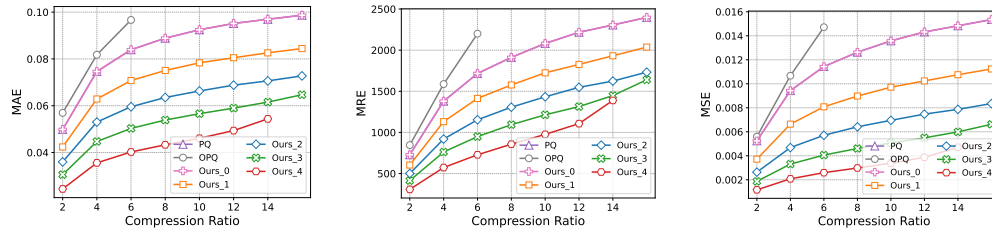


Figure 3: MAE on 8 subspaces. Figure 4: MRE on 8 subspaces. Figure 5: MSE on 8 subspaces.

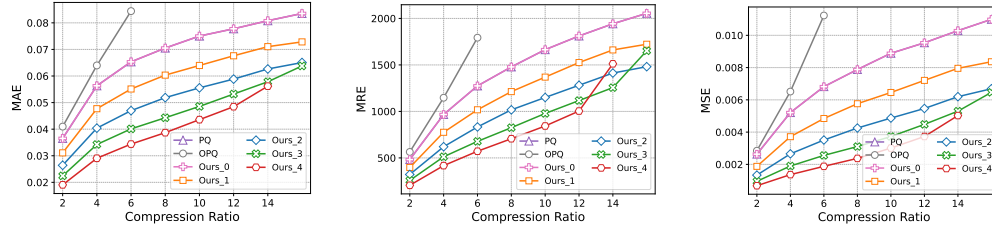


Figure 6: MAE on 16 subspaces. Figure 7: MRE on 16 subspaces. Figure 8: MSE on 16 subspaces.

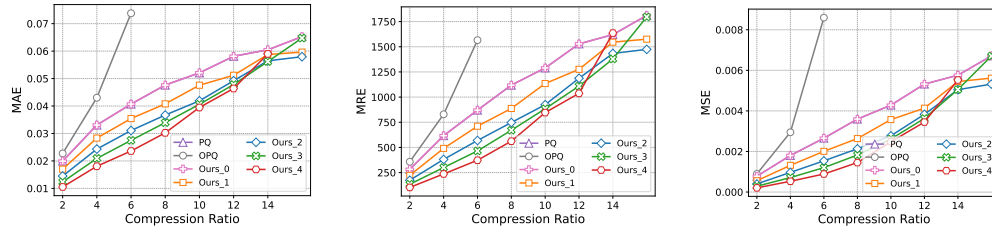


Figure 9: MAE on 32 subspaces. Figure 10: MRE on 32 subspaces. Figure 11: MSE on 32 subspaces.

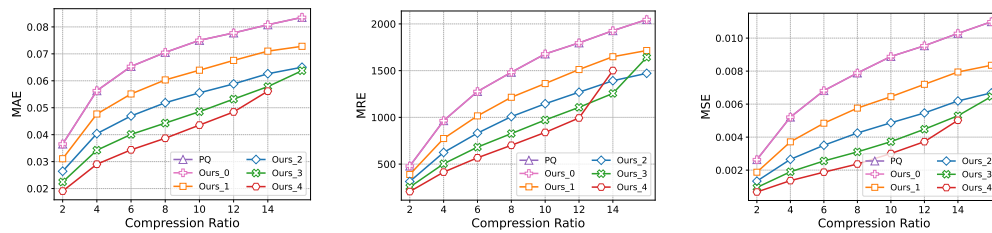


Figure 12: MAE on 128 subspaces. Figure 13: MRE on 128 subspaces. Figure 14: MSE on 128 subspaces.

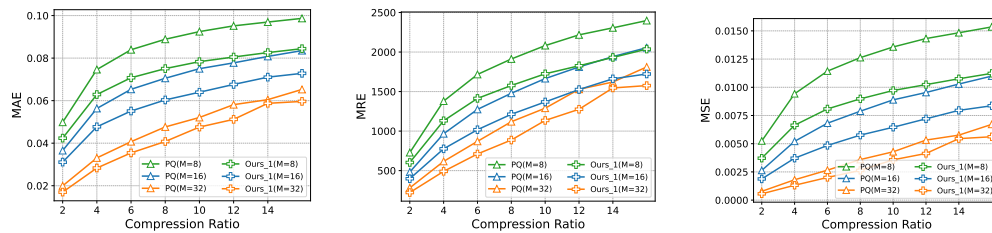


Figure 15: MAE on 1 iterations. Figure 16: MRE on 1 iterations. Figure 17: MSE on 1 iterations.

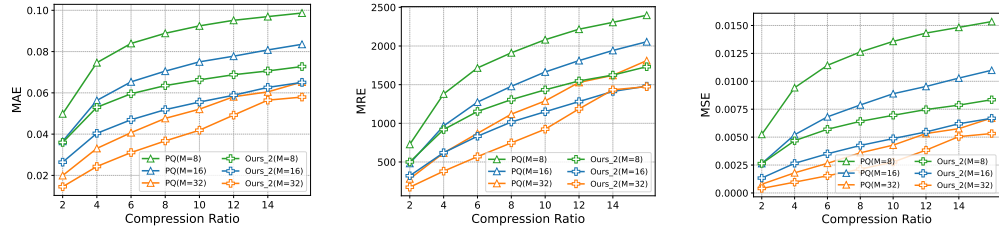


Figure 18: MAE on 2 iterations. Figure 19: MRE on 2 iterations. Figure 20: MSE on 2 iterations.

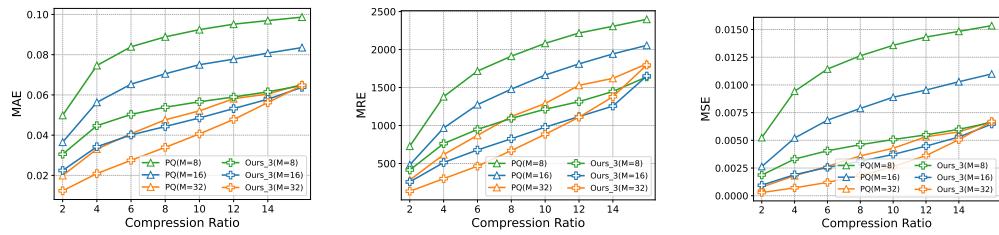


Figure 21: MAE on 3 iterations. Figure 22: MRE on 3 iterations. Figure 23: MSE on 3 iterations.

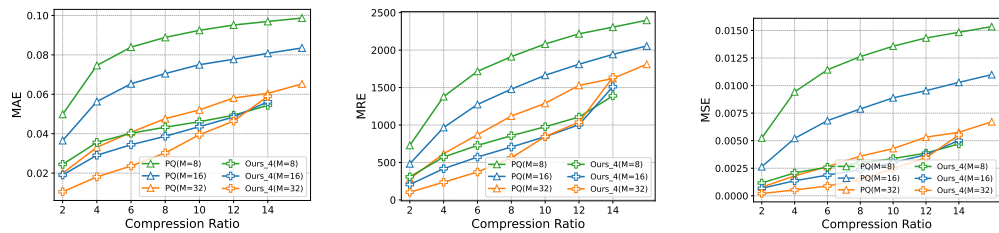


Figure 24: MAE on 4 iterations. Figure 25: MRE on 4 iterations. Figure 26: MSE on 4 iterations.

3- 5, Figures 6- 8, Figures 9- 11, Figures 12- 14 respectively. For 8-subspace setting, HERA can reduce the MSE to 70.4%, 49.7%, 35.1% and 12.3% in 1-4 iterations, respectively.

From the experimental results, we can derive four conclusions. Firstly, the higher the compression ratio, the less space is consumed, but the accuracy decreases. Secondly, the OPQ algorithm performs worse than others with the same compression rate because it needs to store the transformation matrix. Additionally, the PQ algorithm does not perform as well as our improved algorithm. Finally, the more iterations, the better the performance of our algorithm.

We also conducted a parameter sensitivity test under different iterations, evaluating how the number of subspaces affects the algorithm’s performance. The results for 1 to 4 iterations are shown in Figures 15- 17, Figures 18- 20, and Figures 21- 23, respectively. Extensive experiments demonstrate that our algorithm reduces parameter sensitivity, making parameter selection more user-friendly (as indicated by the closer proximity of parameters in our algorithm’s curves).

## 6 FUTURE WORK

In future work, we plan to apply this algorithm to the quantization of large model parameters and the kv cache. This will allow us to evaluate the algorithm’s effectiveness in handling the challenges posed by large-scale models and real-time processing scenarios, further extending its applicability and performance in practical machine learning tasks.

## 7 CONCLUSION

In conclusion, our research addresses critical challenges in the optimization of large language models (LLMs) through the development of a novel algorithm, HERA. The growing complexity and scale of LLMs necessitate innovative approaches to enhance storage and computational efficiency, particularly in vector database management, weight quantization, and key-value (k-v) cache optimization.

HERA’s hierarchical approach to segmenting, compressing, and reorganizing the matrix dataset has proven to be effective in significantly reducing quantization error. By considering the distribution and magnitude of parameters, our method achieves superior performance compared to traditional uniform quantization techniques. The experimental results from our prototype system, implemented in Python, demonstrate that HERA can reduce the quantization error to 12.3% of the original, maintaining the same compression ratio.

Future work will explore further refinements to HERA, including its application to other types of application and broader datasets. Additionally, investigating the integration of HERA with other optimization techniques may yield even greater enhancements in model performance and efficiency. The promising results of this study encourage continued research and development in the quest for more effective and scalable solutions for LLM compression and optimization.

## REFERENCES

- ann-wiki-1m. <https://huggingface.co/datasets/unum-cloud/ann-wiki-1m>, 2023.
- Josh Achiam, Steven Adler, Sandhini Agarwal, Lama Ahmad, Ilge Akkaya, Florencia Leoni Aleman, Diogo Almeida, Janko Altschmidt, Sam Altman, Shyamal Anadkat, et al. Gpt-4 technical report. *arXiv preprint arXiv:2303.08774*, 2023.
- Muhammad Adnan, Akhil Arunkumar, Gaurav Jain, Prashant Nair, Ilya Soloveychik, and Purushotham Kamath. Keyformer: Kv cache reduction through key tokens selection for efficient generative inference. *Proceedings of Machine Learning and Systems*, 6:114–127, 2024.
- Nieves R Brisaboa, Susana Ladra, and Gonzalo Navarro. k2-trees for compact web graph representation. In *International symposium on string processing and information retrieval*, pp. 18–30. Springer, 2009.

- Tom Brown, Benjamin Mann, Nick Ryder, Melanie Subbiah, Jared D Kaplan, Prafulla Dhariwal, Arvind Neelakantan, Pranav Shyam, Girish Sastry, Amanda Askell, et al. Language models are few-shot learners. *Advances in neural information processing systems*, 33:1877–1901, 2020.
- Francisco Claude and Susana Ladra. Practical representations for web and social graphs. In *Proceedings of the 20th ACM international conference on Information and knowledge management*, pp. 1185–1190, 2011.
- Tim Dettmers, Artidoro Pagnoni, Ari Holtzman, and Luke Zettlemoyer. Qlora: Efficient finetuning of quantized llms. *Advances in Neural Information Processing Systems*, 36, 2024.
- Jacob Devlin, Ming-Wei Chang, Kenton Lee, and Kristina Toutanova. Bert: Pre-training of deep bidirectional transformers for language understanding. *arXiv preprint arXiv:1810.04805*, 2018.
- Haojie Duanmu, Zhihang Yuan, Xiuhong Li, Jiangfei Duan, Xingcheng Zhang, and Dahua Lin. Skvq: Sliding-window key and value cache quantization for large language models. *arXiv preprint arXiv:2405.06219*, 2024.
- Elias Frantar, Saleh Ashkboos, Torsten Hoefler, and Dan Alistarh. Gptq: Accurate post-training quantization for generative pre-trained transformers. *arXiv preprint arXiv:2210.17323*, 2022.
- Tiezheng Ge, Kaiming He, Qifa Ke, and Jian Sun. Optimized product quantization. *IEEE transactions on pattern analysis and machine intelligence*, 36(4):744–755, 2013.
- Robert M. Gray and David L. Neuhoff. Quantization. *IEEE transactions on information theory*, 44(6):2325–2383, 1998.
- Coleman Hooper, Sehoon Kim, Hiva Mohammadzadeh, Michael W Mahoney, Yakun Sophia Shao, Kurt Keutzer, and Amir Gholami. Kvquant: Towards 10 million context length llm inference with kv cache quantization. *arXiv preprint arXiv:2401.18079*, 2024.
- Herve Jegou, Matthijs Douze, and Cordelia Schmid. Product quantization for nearest neighbor search. *IEEE transactions on pattern analysis and machine intelligence*, 33(1):117–128, 2010.
- Yannis Kalantidis and Yannis Avrithis. Locally optimized product quantization for approximate nearest neighbor search. In *Proceedings of the IEEE conference on computer vision and pattern recognition*, pp. 2321–2328, 2014.
- Zayd Muhammad Kawakibi Zuhri, Muhammad Farid Adilazuarda, Ayu Purwarianti, and Alham Fikri Aji. Mlkv: Multi-layer key-value heads for memory efficient transformer decoding. *arXiv e-prints*, pp. arXiv–2406, 2024.
- Sehoon Kim, Coleman Hooper, Amir Gholami, Zhen Dong, Xiuyu Li, Sheng Shen, Michael W Mahoney, and Kurt Keutzer. Squeezellm: Dense-and-sparse quantization. *arXiv preprint arXiv:2306.07629*, 2023.
- Woosuk Kwon, Zhuohan Li, Siyuan Zhuang, Ying Sheng, Lianmin Zheng, Cody Hao Yu, Joseph Gonzalez, Hao Zhang, and Ion Stoica. Efficient memory management for large language model serving with pagedattention. In *Proceedings of the 29th Symposium on Operating Systems Principles*, pp. 611–626, 2023.
- Yann LeCun, John Denker, and Sara Solla. Optimal brain damage. *Advances in neural information processing systems*, 2, 1989.
- Yann LeCun, Léon Bottou, Yoshua Bengio, and Patrick Haffner. Gradient-based learning applied to document recognition. *Proceedings of the IEEE*, 86(11):2278–2324, 1998.
- Wonbeom Lee, Jungi Lee, Junghwan Seo, and Jaewoong Sim. {InfiniGen}: Efficient generative inference of large language models with dynamic {KV} cache management. In *18th USENIX Symposium on Operating Systems Design and Implementation (OSDI 24)*, pp. 155–172, 2024.
- Ji Lin, Jiaming Tang, Haotian Tang, Shang Yang, Xingyu Dang, and Song Han. Awq: Activation-aware weight quantization for llm compression and acceleration. *arXiv preprint arXiv:2306.00978*, 2023.

- Ji Lin, Jiaming Tang, Haotian Tang, Shang Yang, Wei-Ming Chen, Wei-Chen Wang, Guangxuan Xiao, Xingyu Dang, Chuang Gan, and Song Han. Awq: Activation-aware weight quantization for on-device llm compression and acceleration. *Proceedings of Machine Learning and Systems*, 6: 87–100, 2024.
- Zichang Liu, Aditya Desai, Fangshuo Liao, Weitao Wang, Victor Xie, Zhaozhao Xu, Anastasios Kyriillidis, and Anshumali Shrivastava. Scissorhands: Exploiting the persistence of importance hypothesis for llm kv cache compression at test time. *Advances in Neural Information Processing Systems*, 36, 2024.
- Qingqun Ning, Jianke Zhu, Zhiyuan Zhong, Steven CH Hoi, and Chun Chen. Scalable image retrieval by sparse product quantization. *IEEE Transactions on Multimedia*, 19(3):586–597, 2016.
- Aude Oliva and Antonio Torralba. Modeling the shape of the scene: A holistic representation of the spatial envelope. *International journal of computer vision*, 42:145–175, 2001.
- Wenqi Shao, Mengzhao Chen, Zhaoyang Zhang, Peng Xu, Lirui Zhao, Zhiqian Li, Kaipeng Zhang, Peng Gao, Yu Qiao, and Ping Luo. Omniquant: Omnidirectionally calibrated quantization for large language models. *arXiv preprint arXiv:2308.13137*, 2023.
- Irene Solaiman, Miles Brundage, Jack Clark, Amanda Askell, Ariel Herbert-Voss, Jeff Wu, Alec Radford, Gretchen Krueger, Jong Wook Kim, Sarah Kreps, et al. Release strategies and the social impacts of language models. *arXiv preprint arXiv:1908.09203*, 2019.
- Antonio Torralba, Rob Fergus, and William T Freeman. 80 million tiny images: A large data set for nonparametric object and scene recognition. *IEEE transactions on pattern analysis and machine intelligence*, 30(11):1958–1970, 2008.
- Hugo Touvron, Louis Martin, Kevin Stone, Peter Albert, Amjad Almahairi, Yasmine Babaei, Nikolay Bashlykov, Soumya Batra, Prajjwal Bhargava, Shruti Bhosale, et al. Llama 2: Open foundation and fine-tuned chat models. *arXiv preprint arXiv:2307.09288*, 2023.
- Guangxuan Xiao, Ji Lin, Mickael Seznec, Hao Wu, Julien Demouth, and Song Han. Smoothquant: Accurate and efficient post-training quantization for large language models. In *International Conference on Machine Learning*, pp. 38087–38099. PMLR, 2023.
- Donna Xu, Ivor W Tsang, and Ying Zhang. Online product quantization. *IEEE Transactions on Knowledge and Data Engineering*, 30(11):2185–2198, 2018.
- Tan Yu, Junsong Yuan, Chen Fang, and Hailin Jin. Product quantization network for fast image retrieval. In *Proceedings of the European Conference on Computer Vision (ECCV)*, pp. 186–201, 2018.
- Yuxuan Yue, Zhihang Yuan, Haojie Duanmu, Sifan Zhou, Jianlong Wu, and Liqiang Nie. Wkvquant: Quantizing weight and key/value cache for large language models gains more. *arXiv preprint arXiv:2402.12065*, 2024.
- Zhenyu Zhang, Ying Sheng, Tianyi Zhou, Tianlong Chen, Lianmin Zheng, Ruisi Cai, Zhao Song, Yuandong Tian, Christopher Ré, Clark Barrett, et al. H2o: Heavy-hitter oracle for efficient generative inference of large language models. *Advances in Neural Information Processing Systems*, 36, 2024.